

Effect of cylinder wall temperature on marine engine combustion

Kweon Ha Park[†]

(Received December 11, 2023 : Revised December 18, 2023 : Accepted December 18, 2023)

Abstract: With the strengthening of fuel-efficiency regulations for marine engines, many studies are underway to enhance their efficiency. To achieve greater fuel efficiency, ship operating speeds are reduced. However, a reduction in the ship speed significantly lowers the temperature of the cylinder liner wall, leading to increased heat loss owing to the enhanced heat transfer to the cooling water. This study presents a detailed analysis of the effect of the surface temperature of the cylinder liner in long-stroke marine engines on fuel spray and combustion. A detailed analysis is conducted on the effect of the surface temperature of the cylinder liner in a slow-speed marine engine on fuel spray and combustion. This study analyzes parameters such as the penetration and distribution of the fuel spray, variations in the combustion speed, distribution of OH radicals representing the combustion boundary layer, and the generation processes of combustion products such as NO and CO. The analysis indicates that, for a comprehensive consideration of combustion efficiency and exhaust emissions, maintaining the cylinder liner wall temperature within the range of 150 to 180 °C is desirable.

Keywords: Marine engine, Cylinder wall temperature, Combustion efficiency, Exhaust emissions

1. Introduction

Regulations on the emissions, including carbon dioxide and nitrogen oxides, from maritime vessels are undergoing increased scrutiny. Carbon dioxide, a major greenhouse gas, was mandated through the Energy Efficiency Existing Ship Index at the 62nd session of the International Maritime Organization's Marine Environment Protection Committee. This initiative has officially commenced with a targeted reduction of over 50% compared to the 2008 levels by 2050 [1]-[3]. Similarly, regulations on nitrogen oxides were substantially reinforced in the progressive stages [4]-[5].

In response to these heightened regulations, numerous new technologies have been developed and implemented. However, there is a shortage of technological advancements on existing ships. Research on the temperature of cylinder liners has been conducted as part of the efforts to enhance the performance of traditional ship engines. This study investigated the heat transfer characteristics, lubrication properties, and engine performance.

Numerous studies have been conducted on the influence of cylinder wall temperature variations on the heat transfer characteristics between the wall and combustion gases. Research predicting the cylinder wall temperature based on the cylinder pressure changes per cycle has been conducted through heat transfer

analysis. The predicted data from this analysis were used for engine control. The accuracy of the thermodynamic cycle analysis was enhanced by applying a wall temperature heat transfer model and interpreting the gas temperature changes at the boundary surface [6]-[7]. Research has been conducted on the instantaneous heat transfer to the cylinder wall. Studies have been conducted by measuring the phenomenon of instantaneous heat transfer in a four-stroke experimental engine and calculating the effects of the temperature profiles [8]-[10]. A study was conducted on the vibration of the wall temperature in diesel engines to determine the impact of periodic temperature changes on wall materials [11]. This study demonstrated that in an indirect-injection diesel engine, the heat transfer characteristics between the cylinder wall and gas are significantly dependent on the engine speed and load with respect to the crank angle [12]-[13].

Research has been conducted on the impact of the wall temperature on the lubrication performance and cylinder wear. The cylinder wall temperature is a crucial factor for the efficiency and engine lifetime. Excessively high temperatures can damage the lubricating film, reducing the engine lifespan and efficiency, while excessively low temperatures can also adversely affect the engine performance. Therefore, to enhance the engine lifespan and performance, it is essential to appropriately control the tem-

[†] Corresponding Author (ORCID: <https://orcid.org/0000-0001-9460-8399>): Professor, Division of Mechanical Engineering, Korea Maritime & Ocean University, 727, Taejong-ro, Yeongdo-gu, Busan 49112, Korea, E-mail: khpark@kmou.ac.kr, Tel: +82-51-410-4367

This is an Open Access article distributed under the terms of the Creative Commons Attribution Non-Commercial License (<http://creativecommons.org/licenses/by-nc/3.0>), which permits unrestricted non-commercial use, distribution, and reproduction in any medium, provided the original work is properly cited.

perature of the cylinder wall [14]-[15]. Research has been conducted on the effect of the wall temperature on engine oil consumption. Oil consumption is primarily caused by oil evaporation from the cylinder wall, which is closely related to the wall temperature [16]. The cylinder wall temperatures were measured using a single-cylinder engine. This study specifically focused on cold-running conditions, highlighting that rapid wear occurs when the temperature drops below a certain threshold [17]-[19]. The influence of the cylinder wall temperature on the engine performance was investigated. In homogeneous charge compression ignition (HCCI) engines, the cylinder wall temperature was studied as a critical factor in determining the combustion timing. The variations in the wall temperature significantly affected the combustion duration, heat transfer, and combustion efficiency. Research has been conducted to control the amount of residual gas to maintain an appropriate wall temperature [20]-[21]. The impact of the cylinder wall temperature on the combustion in diesel engines has also been evaluated. The highest heat transfer occurred during the main combustion period when high-temperature flames were present, which significantly affected the engine efficiency and energy discharge [22]. Studies have been conducted on the effect of the wall temperature on the performance of Atkinson engines. The impact on the output was measured by varying the compression ratio. Increasing the cylinder temperature at all compression ratios resulted in an increased output [23]. The influence of the wall temperature on the engine performance during the transition region in diesel engines was investigated. It was confirmed that the increase in the engine speed with increasing load is a function of the wall temperature [24].

With the increasing stringency of fuel efficiency regulations for ships, there has been a growing interest in maritime operational technologies. Ships reduce their speeds to enhance fuel efficiency. However, a decrease in the ship speed significantly lowers the temperature of the cylinder liner, leading to increased heat loss owing to enhanced heat transfer to the cooling water. To address this issue, research has been conducted on the impact of the temperature control of the cylinder liner on energy efficiency improvement [25]. However, studies analyzing the influence of the cylinder wall temperature on the combustion process and combustion products in marine engines are currently limited.

This study presents a detailed analysis of the effect of the surface temperature of a cylindrical liner in long-stroke marine engines on fuel injection and combustion. The analysis covers pa-

rameters such as the fuel spray distance and distribution, variations in the combustion speed and pressure, distribution of OH radicals representing the combustion boundary layer, and generation and elimination processes of combustion products such as NO and CO.

2. Mathematical Model and Calculation Conditions

The objective of this study was to analyze the combustion behavior inside a cylinder to improve the performance of ship engines. To achieve this, the KIVA code, which is a widely used commercial code for internal combustion engine simulations, was employed. The code was validated by comparing its models for engine combustion, spray, and turbulence with experimental results [26],[27]. Additionally, the influence of the grid was evaluated [28]. The code was applied to engine combustion by comparing the computed results with experimental data for swirl and turbulent flow, spray and combustion, cylinder pressure variations, heat release rate, soot, and nitrogen oxide generation. The results were validated and demonstrated good agreement with the experimental data [29]-[30]. This validated code has been utilized for the development and improvement of numerous diesel engines [31]-[32].

2.1 Mathematical Model

The transport equations used in this analysis are as follows [33].

The continuity equation for the chemical species m is given by **Equation (1)**.

$$\frac{\partial \rho_m}{\partial t} + \nabla \cdot (\rho_m u) = \nabla \cdot [\rho D \nabla \left(\frac{\rho_m}{\rho} \right)] + \dot{\rho}_m^c + \dot{\rho}_m^s \delta_{m1} \quad (1)$$

where ρ_m is the mass density of the species m , ρ is the overall mass density, u is the flow velocity, and D is the diffusivity.

The continuity equation for the entire fluid encompassing all the chemical species is given by **Equation (2)**.

$$\frac{\partial \rho}{\partial t} + \nabla \cdot (\rho u) = \dot{\rho}^s \quad (2)$$

The momentum equation is given by **Equation (3)**.

$$\frac{\partial (\rho u)}{\partial t} + \nabla \cdot (\rho u u) = -\frac{1}{\alpha^2} \nabla p - A_o \nabla^2 / 3 \rho k + \nabla \cdot \sigma + F^s + \rho \quad (3)$$

where, the viscous stress tensor is given by **Equation (4)**.

$$\sigma = \mu[\nabla u + (\nabla u)^T] + \lambda \nabla \cdot u \quad (4)$$

where μ and λ are the 1st and 2nd viscosity coefficients, respectively.

The internal energy equation is given by **Equation (5)**.

$$\frac{\partial(\rho I)}{\partial t} + \nabla \cdot (\rho u I) = -\rho \nabla \cdot u + (I - A_o)\sigma : \nabla u - \nabla \cdot J + A_o \rho \varepsilon + \dot{Q}^c + \dot{Q}^s \quad (5)$$

Here, the heat flux J is given as follows.

$$J = -K \nabla T - \rho D \sum_m h_m \nabla \left(\frac{\rho m}{\rho} \right) \quad (6)$$

The turbulent kinetic energy and its dissipation rate are expressed by **Equations (7) and (8)**, respectively.

$$\frac{\partial(\rho k)}{\partial t} + \nabla \cdot (\rho u k) = -\frac{2}{3} \rho k \nabla \cdot u + \sigma : \nabla u + \nabla \cdot \left[\left(\frac{\mu}{\rho r_k} \right) \nabla k \right] - \rho \varepsilon + \dot{W}^s \quad (7)$$

$$\frac{\partial(\rho \varepsilon)}{\partial t} + \nabla \cdot (\rho u \varepsilon) = -\left(\frac{2}{3} c_{\varepsilon 1} - c_{\varepsilon 3} \right) \rho \varepsilon \nabla \cdot u + \nabla \cdot \left[\left(\frac{\mu}{\rho r_\varepsilon} \right) \nabla \varepsilon \right] + \frac{\varepsilon}{k} [c_{\varepsilon 1} \sigma : \nabla u - c_{\varepsilon 2} \rho \varepsilon + c_s \dot{W}^s] \quad (8)$$

2.2 Calculation Conditions

Figure 1 shows the grid configuration at a crank angle of 30°. This grid was generated by inputting the combustion chamber geometry data of the target engine into K3VPREP, with a total of 28,300 grids.

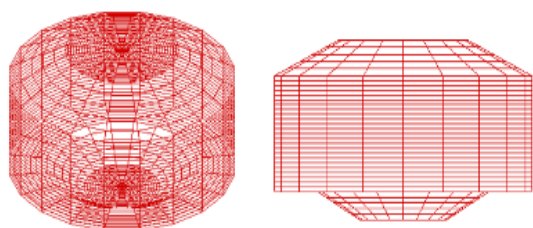


Figure 1: Calculation grids at ATDC 30

Table 1 lists the engine specifications and computational conditions. The target engine is a long-stroke diesel engine with a stroke-to-bore ratio of 3.2. The engine load was set at 70% of the Maximum Continuous Rating (MCR), corresponding to 500 kW/cylinder, considering typical operating loads for marine engines. The analysis focused on the influence of the cylinder wall temperature on the combustion behavior to improve the engine

performance through cooling water control. The wall temperatures used in the calculations vary from 90 to 210 °C at intervals of 30 °C. For more detailed information, please refer to **Table 1**.

Table 1: Engine specifications and calculation conditions

Cases	Parameter	Value	Unit
Target engine & conditions	Type of target engine	2-stroke cycle	-
	Operating output	500	kW/cyl
	Engine speed	180	rpm
	Bore x Stroke	42x136	cm
	Crank angle at compression start	ATDC 120	CA
	Crank angle at exhaust valve open	BTDC 120	CA
	Number of nozzle hole	1	EA
	Mass flow of fuel injection per stroke	8	g/stroke
	Fuel injection pressure	40	MPa
	Fuel spray angle	30	deg
	Injection duration	10	CA
	Wall temperature	150	°C
	Initial air temperature	60	°C
Initial air pressure	0.15	MPa	
Length of connecting rod	182	cm	
Compression ratio	28.6	-	
Cylinder liner wall temperature	Temperature	90	°C
		120	°C
		150	°C
		180	°C
		210	°C

3. Results and Discussion

3.1 Fuel Spray Behavior

Figure 2 shows the fuel distribution at various crank angles as the cylinder liner wall temperature varies from 90 to 210 °C. The injected fuel propagates towards the center of the combustion chamber until the end of the injection, simultaneously undergoing evaporation and combustion at the spray boundary. When the wall temperature is 90 °C, the fuel propagates the farthest, and at 150 and 180 °C, the propagation distance decreases, resulting in a wider dispersion vertically. However, when the wall temperature increases to 210 °C, the propagation distance increases again. This phenomenon is more pronounced when the crank angle is 10°. In all cases, except for the wall temperature of 180 °C, the fuel reaches the piston crown, exhibiting behavior where it adheres to the upper piston wall. The fuel distributed on the piston wall at lower temperatures resulted in a slower combustion rate as the piston descended. The amount of residual fuel until

the exhaust valve opens at an ATDC of 120° depends on the fuel formed near the piston wall. A wall temperature of 180 °C, which forms a fuel distribution in the cylindrical space above the piston crown, results in less residual fuel.

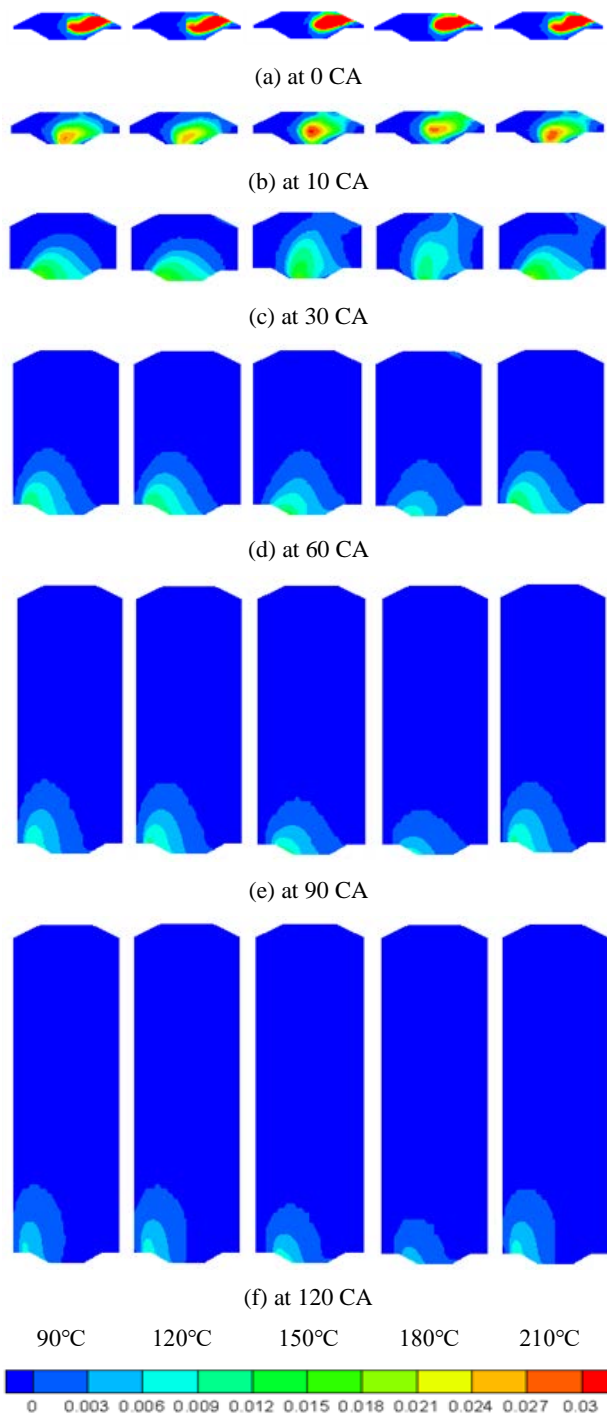


Figure 2: Fuel (C16H34) distribution on the center section

Figure 3 depicts the variation in the residual fuel mass with the crank angle as the cylinder wall temperature ranges from 90

to 210 °C. For wall temperatures below 120 °C, where rapid combustion occurs during the fuel injection period, the reduction rate of the residual fuel slows down as the piston expands, and the combustion rate sharply decreases. However, for a wall temperature of 180 °C, there was a significant reduction in the residual fuel. However, when the wall temperature increases to 210 °C, the reduction rate of residual fuel slows down again. As observed in the mentioned phenomena, the amount of burned fuel at an ATDC of 120°, the moment when the exhaust valve opens, is highest at a wall temperature of 180 °C. If the wall temperature was either higher or lower than 180 °C, the amount of burned fuel decreased (Figure 4).

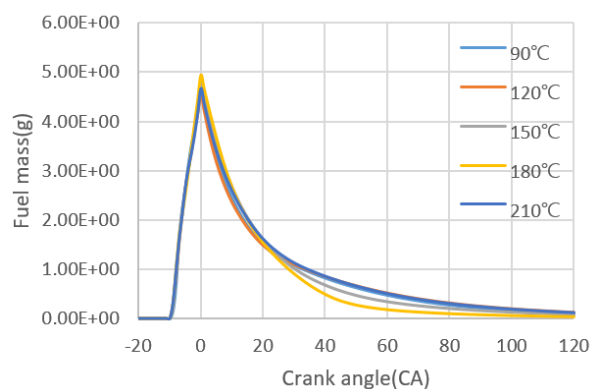


Figure 3: Residual fuel mass with wall temperature variation

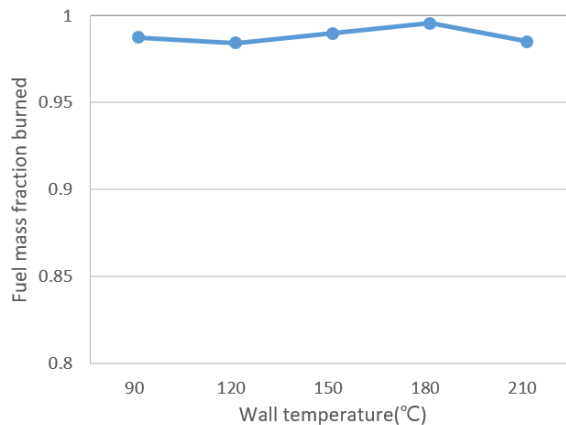


Figure 4: Fuel mass fraction burned at the exhaust valve open with wall temperature variation

3.2 Flame Propagation and Behavior

Figure 5 illustrates the distribution of the OH radicals forming the flame front. During fuel injection, the slow evaporation of the injected fuel spray extends the flame to a greater distance at

lower wall temperatures of 90 °C. As the wall temperature increases to 180 °C, the flame propagation slows down. However, after the main combustion starting at ATDC 10, the most vigorous combustion patterns are observed at 150 °C and 180 °C, showing extensive combustion across a wide area. When the wall temperature was lower than 120 °C or higher than 210 °C, the combustion area moved closer to the piston wall, resulting in a reduced combustion area. The residual amount of OH radicals after combustion, occurring after the exhaust valve opening at ATDC 120°, was also the lowest at a wall temperature of 150 °C, followed by a lower value at 180 °C. (Figure 6).

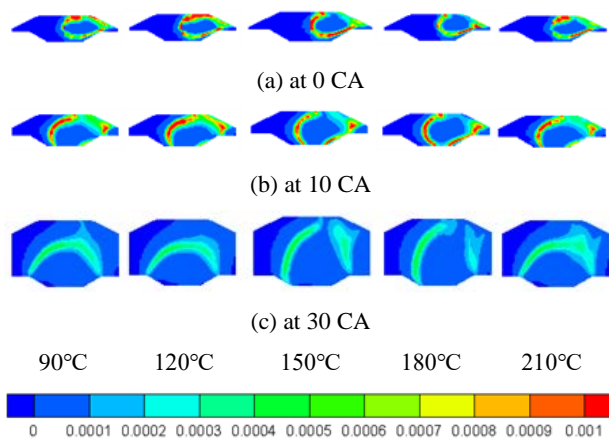


Figure 5: OH radical distributions on the center section

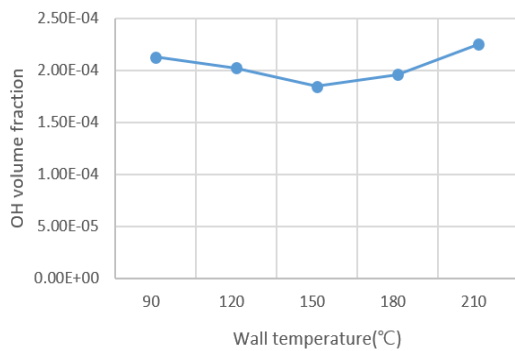


Figure 6: OH radical volume fraction at exhaust valve open with wall temperature variation

3.3 Carbon Monoxide Generation Behavior

Figure 7 shows the behavior of the intermediate combustion product, carbon monoxide (CO), in terms of its generation and extinction. A significant amount of CO is generated up to ATDC 10° when combustion is most active, and it is extinguished as it undergoes complete combustion to carbon dioxide after ATDC 30°. In regions with wall temperatures of 150 °C and 180 °C, the

high-concentration zone of CO is significantly reduced. However, in the low-temperature region below 120 °C and the high-temperature region of 210 °C, a high-concentration zone is observed, especially near the piston crown. This pattern persists until ATDC 120°.

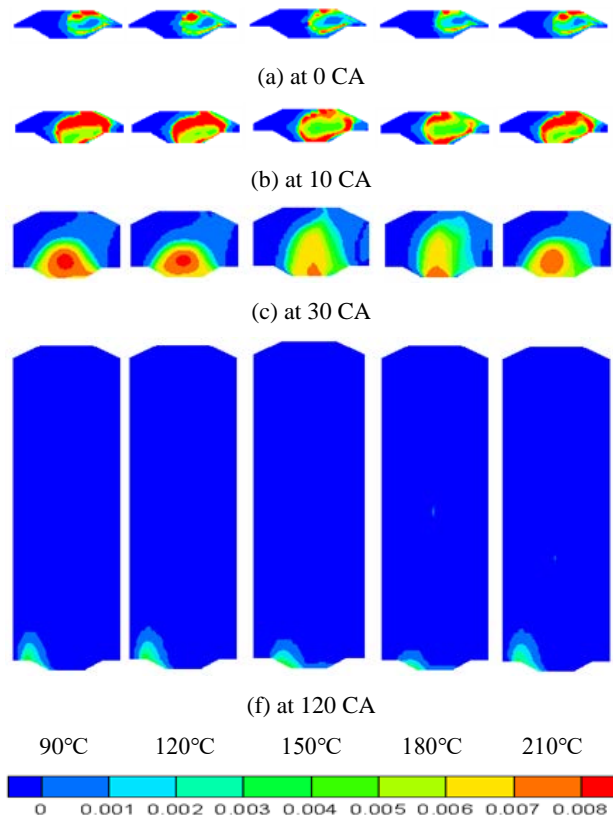


Figure 7: CO distribution at the center section of combustion chamber

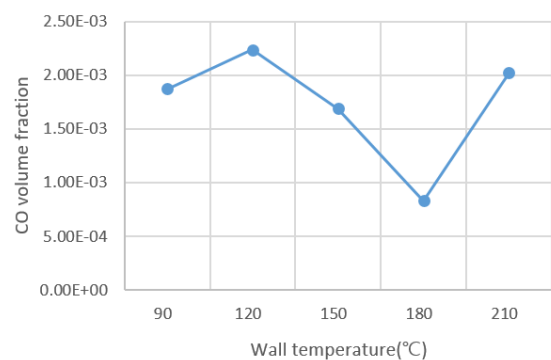


Figure 8: CO volume fraction at the exhaust valve open with wall temperature variation

As shown in Figure 8, at the exhaust valve opening (ATDC 120), the lowest carbon monoxide levels are observed at a wall temperature of 180 °C.

3.4 Nitrogen Oxides Generation Behavior

Figure 9 shows the distribution of nitrogen oxides up to 30° ATDC, where nitrogen monoxide was the most actively generated. Nitrogen monoxide is produced in the high-temperature region downstream of the flame front, and the generated NO rapidly freezes and persists. When the wall temperature is between 150 °C and 180 °C, fuel is widely distributed in the cylinder space, leading to a localized decrease in the flame temperature. Consequently, the rate of nitrogen monoxide generation decreased. At ATDC 120° when the exhaust valve opens, the case with a wall temperature of 180 °C shows the lowest concentration of nitrogen monoxide (**Figure 10**).

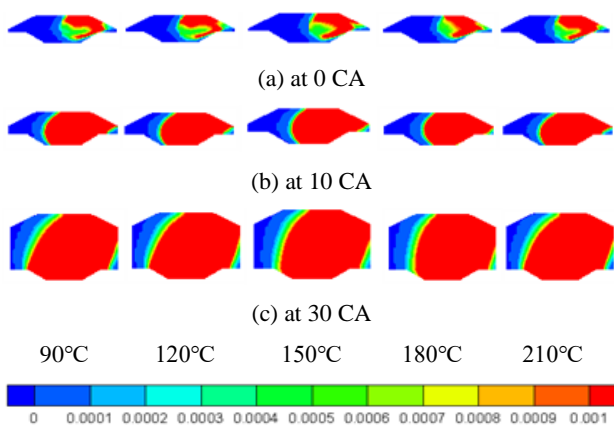


Figure 9: NO distribution at the center section of combustion chamber

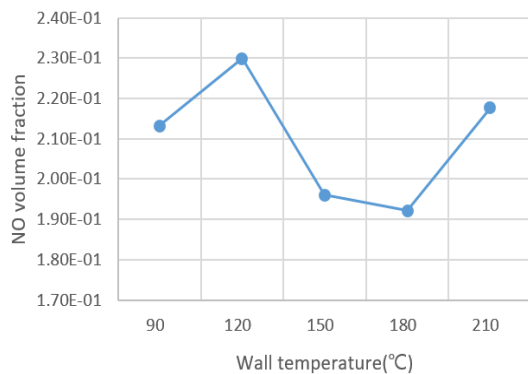


Figure 10: NO volume fraction at the exhaust valve open with wall temperature variation

4. Conclusion

This paper summarized an analysis conducted to enhance the efficiency and reduce exhaust emissions of an operational marine diesel engine by investigating the impact of the cylinder wall temperature on the combustion behavior.

1) The fuel distribution was significant on the lower surface

of the combustion chamber under conditions where the wall temperature was below 150 °C or above 180 °C. Consequently, the amount of unburned fuel that was expelled increased, reaching up to 1.5% at wall temperatures below 120 °C, while remaining below 0.5% at a wall temperature of 180 °C.

- 2) The OH radical, indicating the flame's intensity, exhibited the most vigorous combustion behavior between 150 °C and 180 °C, with combustion progressing over a wide area. When the wall temperature was below 120 °C or above 210 °C, the combustion area shifted near the piston wall, resulting in a reduction in the combustion area. At the moment of the exhaust valve opening, the residual OH radicals, indicative of incomplete combustion, are also at the lowest when the wall temperature is 150 °C.
- 3) When the wall temperature was between 150 °C and 180 °C, the fuel was widely distributed in the cylinder space, resulting in a localized reduction in the flame temperature and hence a decrease in the rate of nitrogen monoxide formation. At the exhaust time, the case with a wall temperature of 180 °C exhibited the lowest concentration of nitrogen oxides.
- 4) Considering the overall combustion efficiency and exhaust emissions, it is desirable to maintain the combustion chamber wall temperature between 150 °C and 180 °C.

Acknowledgements

This work was supported by the Korea Maritime & Ocean University Research Fund in 2022.

Author Contributions

Conceptualization, K. H. Park; Methodology, K. H. Park; Software, K. H. Park; Validation, K. H. Park; Formal Analysis, K. H. Park; Investigation, K. H. Park; Resources, K. H. Park; Data Curation, K. H. Park; Writing—Original Draft Preparation, K. H. Park; Writing—Review & Editing, K. H. Park; Visualization, K. H. Park; Supervision, K. H. Park; Project Administration, K. H. Park; Funding Acquisition, K. H. Park.

References

- [1] FCCC/CP/2015/L.9/Rev.1. United Nations, United Nations Office at Geneva, The United Nations Framework Convention on Climate Change (UNFCCC), Paris, France, 2015.
- [2] V. Masson-Delmotte, P. Zhai, H. O. Pörtner, D. Roberts, J. Skea, P. R. Shukla, A. Pirani, W. Moufouma-Okia, C. Péan,

- R. Pidcock, S. Connors, J. B. R. Matthews, Y. Chen, X. Zhou, M. I. Gomis, E. Lonnoy, T. Maycock, M. Tignor, and T. Waterfield, An IPCC Special Report on the impacts of global warming of 1.5°C above pre-industrial levels and related global greenhouse gas emission pathways, in the context of strengthening the global response to the threat of climate change, sustainable development, and efforts to eradicate poverty, The Intergovernmental Panel on Climate Change(IPCC), 2018.
- [3] Fourth IMO GHG study, International Maritime Organization, London, United Kingdom, 2020.
- [4] A. Azzara, D. Rutherford, and H. Wang, "Feasibility of IMO annex VI tier III implementation using selective catalytic reduction," *The International Council on Clean Transportation*, vol. 4, pp. 1-9, 2014.
- [5] S. Yang, X. Pan, Z. Han, D. Zhao, B. Liu, D. Zheng, and Z. Yan, "Removal of NO_x and SO₂ from simulated ship emissions using wet scrubbing based on seawater electrolysis technology," *Chemical Engineering Journal*, vol. 331, pp. 8-15, 2018.
- [6] F. Yan and J. Wang, "Engine cycle-by-cycle cylinder wall temperature observer-based estimation through cylinder pressure signals," *Journal of Dynamic Systems, Measurement, and Control*, vol. 134, no. 6, 2012. [Online]. Available: <https://doi.org/10.1115/1.4006222>.
- [7] C. D. Rakopoulos, E. G. Giakoumis, and D. C. Rakopoulos, "Study of the short-term cylinder wall temperature oscillations during transient operation of a turbo-charged diesel engine with various insulation schemes," *International Journal of Engine Research*, vol. 9, no. 3, pp. 177-193, 2008. [Online]. Available: <https://doi.org/10.1243/14680874JER00608>.
- [8] C. D. Rakopoulos, D. C. Rakopoulos, G. C. Mavropoulos, and E. G. Giakoumis, "Experimental and theoretical study of the short term, response temperature transients in the cylinder walls of a diesel engine at various operating conditions," *Applied Thermal Engineering*, vol. 24, no. 5-6, pp. 679-702, 2004.
- [9] C. D. Rakopoulos and E. G. Giakoumis, "The influence of cylinder wall temperature profile on the second-law diesel engine transient response," *Applied Thermal Engineering*, vol. 25, no. 11-12, pp. 1779-1795, 2005.
- [10] R. P. Adair, E. B. Qvale, and J. T. Pearson, "Instantaneous heat transfer to the cylinder wall in reciprocating compressors," *International Compressor Engineering Conference*, paper 86, 1972. [Online]. Available: <https://docs.lib.purdue.edu/icec/86>.
- [11] C. D. Rakopoulos, K. A. Antonopoulos, D. C. Rakopoulos and E. G. Giakoumis, "Investigation of the temperature oscillations in the cylinder walls of a diesel engine with special reference to the limited cooled case," *International Journal of Energy Research*, vol. 28, no. 11, pp. 977-1002, 2004. [Online]. Available: DOI: 10.1002/er.1008.
- [12] A. Sanli, A. N. Ozsezen, I. Kilicaslan, and M. Canakci, "The influence of engine speed and load on the heat transfer between gases and in-cylinder walls at fired and motored conditions of an IDI diesel engine," *Applied Thermal Engineering* vol. 28, no. 11-12, pp. 1395-1404, 2008.
- [13] J. Baumgartl, W. Budweiser, G. Mueller, and G. Neumann, "Studies of buoyancy driven convection in a vertical cylinder with parabolic temperature profile," *Journal of Crystal Growth*, vol. 97, no. 1, pp. 9-17, 1989.
- [14] M. O. Teetor, "Cylinder Temperature," SAE Technical Paper, Technical Paper 360130, United States, 1936.
- [15] Z. Ma, N. A. Henein, and W. Bryzik, "A model for wear and friction in cylinder liners and piston rings," *Tribology Transactions*, vol. 49, no. 3, pp. 315-327, 2006.
- [16] M. Soejima, Y. Harigaya, T. Hamatake, and Y. Wakuri, "Study on lubricating oil consumption from evaporation of oil-film on cylinder wall for diesel engine," *SAE International Journal of Fuels and Lubricants*, vol. 10, no. 2, pp. 487-501, 2017.
- [17] C. G. Williams, *Cylinder Wear in Gasoline Engines*, SAE Transactions, vol. 31, pp. 191-196, United States, 1936. [Online]. Available: <https://www.jstor.org/stable/44439103>.
- [18] T. S. Sudarshan and S. B. Bhaduri, "Wear in cylinder liners," *Wear*, vol. 91, no. 3, pp. 269-279, 1983.
- [19] S. Someya, Y. Okura, T. Munakata, and K. Okamoto, "Instantaneous 2D imaging of temperature in an engine cylinder with flame combustion," *International Journal of Heat and Mass Transfer*, vol. 62, pp. 382-390, 2013.
- [20] M. J. Roelle, N. Ravi, A. F. Jungkunz, and J. C. Gerdes, "A dynamic model of recompression HCCI combustion including cylinder wall temperature," *ASME 2006 International Mechanical Engineering Congress and Exposition*, pp. 415-424, 2006. [Online]. Available: <https://doi.org/10.1115/IMECE2006-15125>.
- [21] K. Chang, G. Lavoie, A. Babajimopoulos, and Z. Filipi, "Control of a multi-cylinder HCCI engine during transient

- operation by modulating residual gas fraction to compensate for wall temperature effects,” SAE Technical Paper 2007-01-0204, 2007. [Online]. Available: <https://doi.org/10.4271/2007-01-0204>.
- [22] M. Jia, E. Gingrich, and R. D Reitz, “Effect of combustion regime on in-cylinder heat transfer in internal combustion engines,” *International Journal of Engine Research*, vol. 17, no. 3, pp. 331-346, 2016.
- [23] R. Ebrahimi, “Effects of mean piston speed, equivalence ratio and cylinder wall temperature on performance of an Atkinson engine,” *Mathematical and Computer Modelling*, vol. 53, no. 5-6, pp. 1289-1297, 2011.
- [24] C. D. Rakopoulos, E. G. Giakoumis, and D. C. Rakopoulos, “Cylinder wall temperature effects on the transient performance of a turbocharged diesel engine,” *Energy Conversion and Management*, vol. 45, no. 17, pp. 2627-2638, 2004.
- [25] C. Dere and C. Deniz, “Effect analysis on energy efficiency enhancement of controlled cylinder liner temperatures in marine diesel engines with model based approach,” *Energy Conversion and Management*, vol. 220, 2020.
- [26] S. Singh, R. D. Reitz, and M. P. B. Musculus, T. Lachaux, “Validation of engine combustion models against detailed in-cylinder optical diagnostics data for a heavy-duty compression-ignition engine,” *International Journal of Engine Research*, vol. 8, no. 1, pp. 1-13, 2007.
- [27] S. C. Kong, Z. Han and R. D. Reitz, The Development and Application of a Diesel Ignition and Combustion Model for Multidimensional Engine Simulation, SAE Transactions, *Journal of Engines*, vol. 104, no. 3, pp. 502-518, United States, 1995. [Online]. Available: <https://www.jstor.org/stable/44633235>.
- [28] K. Sone and S. Menon, “Effect of subgrid modeling on the in-cylinder unsteady mixing process in a direct injection engine,” *Journal of Engineering for Gas Turbines and Power*, vol. 125, no. 2, pp. 435-443, 2003. [online]. Available: <https://doi.org/10.1115/1.1501918>.
- [29] R. D. Reitz and C. J. Rutland, “Development and testing of diesel engine CFD models,” *Progress in Energy and Combustion Science*. vol. 21, no. 2, pp. 173-196, 1995. [online]. Available: [https://doi.org/10.1016/0360-1285\(95\)00003-Z](https://doi.org/10.1016/0360-1285(95)00003-Z).
- [30] Y. Jeong, Y. Qian, S. Campbell and K. T. Rhee, Investigation of a Direct Injection Diesel Engine by High-Speed Spectral IR Imaging and KIVA-II, SAE Transactions, *Journal of Engines*, vol. 103, no. 3, pp. 1789-1799, United States, 1994. [Online]. Available: <https://www.jstor.org/stable/44632915>.
- [31] A. Imren, V. Golovitchev, C. Sorousbay and G. Valentino, The Full Cycle HD Diesel Engine Simulations Using KIVA-4 Code, Powertrains Fuels & Lubricants Meeting, San Diego California, United States, 2010. [Online]. Available: <https://doi.org/10.4271/2010-01-2234>.
- [32] D. Wickman, P. Senecal and R. D. Reitz, Diesel Engine Combustion Chamber Geometry Optimization Using Genetic Algorithms and Multi-Dimensional Spray and Combustion Modeling, SAE Transactions, *Journal of Engines*, vol. 110, no. 3, pp. 487-507, United States, 2001. [Online]. Available: <https://www.jstor.org/stable/44724325>.
- [33] A. A. Amsden, P. J. O'Rourke, and T. D. Butler, “KIVA-II: A computer program for chemically reactive flows with sprays,” LA-11560-MS, Los Alamos, New Mexico, 1989.